Modulation of MutS ATP Hydrolysis by DNA Cofactors†

Keith P. Bjornson,‡ Dwayne J. Allen,‡ and Paul Modrich*,§

Department of Biochemistry and Howard Hughes Medical Institute, Duke University Medical Center, Durham, North Carolina 27710

Received October 4, 1999

ABSTRACT: *Escherichia coli* MutS protein, which is required for mismatch repair, has a slow ATPase activity that obeys Michalelis−Menten kinetics. At 37 °C, the steady-state turnover rate for ATP hydrolysis is 1.0 ± 0.3 min^{-1} per monomer equivalent with a K_m of 33 ± 6 μM. Hydrolysis is competitively inhibited by the ATP analogues AMPPNP and ATPγS, with K_i values of 4 μM in both cases, and by ADP with a K_i of 40 μM. The rate of ATP hydrolysis is stimulated 2−5-fold by short hetero- and homoduplex DNAs. The concentration of DNA cofactor that yields half-maximal stimulation is lowest for oligodeoxynucleotide duplexes that contain a mismatched base pair. Pre-steady-state chemical quench analysis has demonstrated a substoichiometric initial burst of ADP formation by free MutS that is governed by a rate constant of 78 min^{-1}, indicating that the rate-limiting step for the steady-state reaction occurs after hydrolysis. Prebinding of MutS to homoduplex DNA does not alter the burst kinetics or amplitude but only increases the steady-state rate. In contrast, binding of the protein to heteroduplex DNA abolishes the burst of ADP formation, indicating that the rate-limiting step now occurs before hydrolysis. Gel filtration analysis indicates that the MutS dimer assembles into higher order oligomers in a concentration-dependent manner, and that ATP binding shifts this equilibrium to favor assembly. These results, together with kinetic findings, indicate nonequivalence of subunits within a MutS oligomer with respect to ATP hydrolysis and DNA binding.

Escherichia coli MutS[1] plays a critical role in the initiation of bacterial mismatch repair (*1*−*3*), a mutation avoidance system that corrects DNA biosynthetic errors and blocks genetic exchange between diverged DNA sequences (*4*, *5*). Mismatch repair systems similar to the bacterial pathway have been identified in a variety of eukaryotes including fungi, insects, amphibians, mouse, and mammals, where they are believed to play an important role in genetic stability (*6*−*8*).

Repair by the *E. coli* pathway is initiated by the binding of MutS to a mismatch (*9*−*11*). MutL binds to heteroduplex DNA in a MutS-dependent manner (*11*−*13*). Assembly of the MutS•MutL•heteroduplex complex is sufficient to activate the d(GATC) endonuclease activity of MutH, which incises the newly synthesized strand at an unmethylated d(GATC) sequence (*1*), and to activate DNA helicase II (*2*), which enters the helix at the incised d(GATC) sequence (*3*). DNA unwinding by helicase II proceeds toward the mismatch, and that portion of the incised strand that is displaced by the helicase is subject to degradation by one of several single-strand-specific exonucleases (*14*, *15*). The resulting gap is repaired by DNA polymerase III holoenzyme in the presence of single-strand DNA binding protein, and DNA ligase restores covalent continuity to the repaired strand (*16*).

A key feature of the bacterial repair system, which is conserved in mammalian cells, is a bidirectional capability; i.e., the strand break that serves as the initiation site for excision may be located either 3′ or 5′ to the mispair on the incised strand (*14*, *17*, *18*). This implies orientation-dependent activation of a 3′ → 5′ or 5′ → 3′ excision system at the strand break. In the case of the *E. coli* system, directional excision has been attributed to orientation-dependent activation of DNA helicase II such that unwinding occurs toward the mispair from the strand break (*3*). Excision has been shown to terminate at a number of sites about 50 nucleotides beyond the original location of the mismatch, but the events involved in termination have not been defined (*15*). The bidirectional excision capability of mismatch repair requires establishment of the relative orientation of the mismatch and the strand signal on the DNA molecule, an effect that requires signal transmission between the two DNA sites along the helix contour. Several lines of evidence have implicated action of the MutS-associated ATPase in this effect.

MutS activities isolated from *E. coli*, *Thermus aquaticus*, and *Thermus thermophilus* exist in solution predominantly as dimers and tetramers (*19*−*21*). The dimer has been shown to be sufficient for mismatch recognition by the *E. coli* and *T. aquaticus* proteins in the absence of ATP (*11*, *21*), although higher order aggregates have been observed by electron microscopy of *E. coli* MutS•DNA complexes at high protein to DNA ratios in the presence of ATP (*11*). DNase I and chemical footprinting experiments have indicated that mismatch recognition by bacterial MutS is associated with

† Supported by Grant GM23719 from the National Institute of General Medical Sciences. P.M. is an Investigator of the Howard Hughes Medical Institute.

* Corresponding author. Tel: (919) 684-2775, Fax: (919) 681-7874, e-mail: modrich@biochem.duke.edu.

‡ Department of Biochemistry.

§ Howard Hughes Medical Institute.

[1] Abbreviations: MutS, product of the bacterial *mutS* gene; kDa, kilodalton(s); BSA, bovine serum albumin; AMPPNP, 5′-adenylyl imidodiphosphate; ATPγS, adenosine 5′-*O*-(3-thiotriphosphate).

10.1021/bi992286u CCC: $19.00 © 2000 American Chemical Society
Published on Web 02/22/2000

protection of about 20 base pairs (*9, 12, 22*), and that the affinity of the protein for the eight possible base−base mismatches varies in the range of $K_{d(G-T)} = 40$ nM for the most tightly bound mispair to $K_{d(C-C)} = 500$ nM for the weakest interaction (*9*). MutS has also been shown to have a modest affinity for nonspecific homoduplex DNA (*23*).

Members of the MutS family also have a Walker A nucleotide binding consensus motif near their carboxyl termini, and an ATPase activity copurifies with bacterial and eukaryotic MutS activities (*1, 24*−*29*). The importance of the MutS ATPase was demonstrated by the finding that genetic inactivation of the nucleotide binding site can confer a dominant negative phenotype in vivo (*24, 30*). The presence of ATP reduces the efficiency of mismatch binding by bacterial MutS and eukaryotic MutSα (*12, 26, 27, 31*−*33*), and ATP challenge of preformed MutS·heteroduplex or MutSα·heteroduplex complexes results in release of the protein from the mismatch (*11, 29, 34*). Since ATPγS results in release of bacterial MutS and eukaryotic MutS homologues from a mismatch (*11, 27, 34*), some of these effects may be attributable to nucleotide binding.

Electron microscopy of complexes between *E. coli* MutS and 6400 base pair heteroduplex DNAs containing a single mismatch demonstrated that ATP-induced release of MutS from a mismatch is associated with movement of the protein along the helix. Upon challenge with ATP, MutS·DNA complexes are converted to α-shaped DNA loop structures that are stabilized by MutS at the base, with the mismatch in most cases internal to the loop (*11*). Loop formation visualized in this manner depends on the presence of a mismatch, and loop size increases in an approximately linear fashion with time. These observations, coupled with the findings that ATPγS fails to support efficient loop formation and addition of excess AMPPNP attenuates ongoing loop growth, led to the suggestion that MutS leaves the mismatch via bidirectional movement along the helix, with movement dependent on ATP hydrolysis (*11*). MutS movement in this manner would be sufficient to couple mismatch recognition to loading of the excision system at the strand break that directs repair (*2, 3*), a site that can be located hundreds of base pairs from this mismatch. Despite an earlier suggestion to the contrary (*26*), it is now clear that mammalian MutSα also leaves the mismatch by movement along the helix contour in an ATP-dependent reaction (*29, 34*). However, in this case the requirement for ATP hydrolysis by DNA-bound MutSα is controversial. The ATP hydrolytic rate by known MutS homologues is quite modest, and although it is difficult to reconcile directional movement with a low ATP hydrolytic rate, a mechanism has been proposed that supports directional movement with only limited energy input (*29*).

To further clarify the role of ATP hydrolysis in MutS function, we have examined nucleotide hydrolysis by the *E. coli* protein using steady-state and pre-steady-state methods. We show that the apparent affinity of the protein for a DNA cofactor is highest when a mismatched base pair is present. While homoduplex and heteroduplex DNAs both activate steady-state ATP hydrolysis by the protein, pre-steady-state analysis indicates that the kinetic mechanism of nucleotide hydrolysis depends on the type of DNA cofactor. We also show that MutS dimers can self-assemble into an higher oligomeric state in a reaction that is facilitated by the binding of ATP.

MATERIALS AND METHODS

Proteins and DNAs. *E. coli* MutS, purified as described (*19*), was greater than 98% pure and stored as a concentrated stock (236 μM) in 50 mM KPO_4, pH 7.4, 150 mM KCl, 1 mM 2-mercaptoethanol, 50% (v/v) glycerol at −20 °C. MutS concentration was determined from the absorbance at 280 nM using an extinction coefficient of 69 420 M^{-1} cm^{-1} calculated from the primary amino acid sequence (*35*). Residual nucleotide present in purified preparations (0.15 mol of ADP/mol of MutS monomer) was determined as previously described (*29*). Nucleotide-free preparations (<0.03 mol of ADP/mol) were prepared by filtration through Sephadex G-50 spin columns (*29*).

Oligonucleotides (Oligo's Etc. Inc., Wilsonville, OR) were further purified using polyacrylamide gel electrophoresis in the presence of 7 M urea. The 50mer DNAs used in this study were comprised of d(TCGCCGAATTGCTAGCAAGCT**T**TCGAGTCTAGAAATTCGGCTTTCCCCGT) hybridized to a perfect complement for control homoduplex, or to a 50mer that was complementary with the exception of placement of G opposite a centrally located thymine (boldface type) for the corresponding heteroduplex. The 20mer substrates were derived from internal sequences of the 50mers above. A 20mer homoduplex was prepared by hybridization of d(TAGCAAGCT**T**TCGAGTCTAG) to its complement, while a G−T heteroduplex was prepared by hybridization to a 20mer that was complementary with the exception of placement of a G opposite the central T indicated in boldface. Oligonucleotides were annealed in 10 mM Tris-HCl, pH 8.0, 100 mM KCl, and 1 mM EDTA at 90 °C and cooled slowly to room temperature. Concentrated stock solutions (10 μM) were stored at 4 °C. The 31 base pair G−T heteroduplex used for gel shift binding assay has been previously described (*11*).

Gel Shift Assay for MutS·DNA Complex Formation. Reactions (20 μL) contained 50 mM Tris-HCl (pH 7.4), 20 mM KCl, 1 mM dithiothreitol, 0.5 mM $MgCl_2$, 1 pmol of a 5′-^{32}P-end-labeled 31 base pair G−T heteroduplex, and nucleotide-free MutS as indicated. After incubation at 25 °C for 10 min, reactions were supplemented with 2 μL of 40% sucrose and subjected to electrophoresis through 6% polyacrylamide gels in 40 mM Tris−acetate (pH 7.2), 1 mM EDTA at 10 V/cm for 2.5 h. Gels were pre-run for 30 min prior to sample application. After electrophoresis, gels were dried under vacuum, and DNA was visualized by Phosphoimager analysis (Molecular Dynamics, Sunnyvale, CA).

Steady-State and Pre-Steady-State Kinetics. The steady-state rate of ATP hydrolysis by MutS was measured at 37.0 °C in 25 mM Tris-HCl, pH 7.6, 20 mM KCl, 5 mM $MgCl_2$, 1 mM dithiotheitol, and 100 μg/mL BSA in a final volume of 20 μL. A MutS working stock (1 mL of 1.2 μM) was prepared from the concentrated protein stock by dilution into assay buffer. The steady-state ATPase data shown within a figure panel were all performed on the same day with the same MutS protein dilution. Reactions were assembled on ice (MutS, DNA, and nucleotide analogues as indicated) and incubated for a minimum of 5 min at 37 °C prior to the addition of [α-^{32}P]ATP (2500 μCi/mmol) to initiate the reaction. Initial rate determinations were based on removal of samples (2 μL) as a function of time, which were quenched with 50 μL of 0.5 M EDTA, pH 8.0. The extent

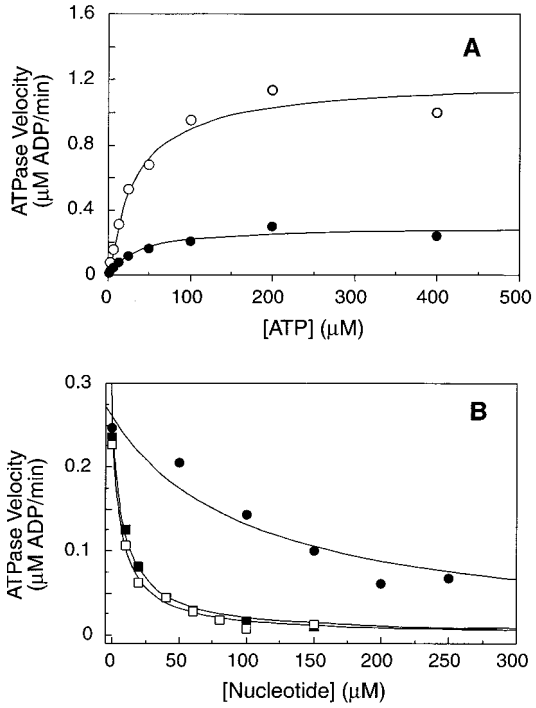

FIGURE 1: MutS ATPase activity is stimulated by mismatched DNA. Steady-state ATPase experiments were performed as described under Materials and Methods at a MutS concentration of 300 nM MutS (monomer concentration). ATP concentration was varied as indicated. (Panel A) ATPase activity in the absence (●) or presence (○) of 1 μM 20 base pair G−T heteroduplex. Curves shown are nonlinear least-squares regression fit [Marquardt algorithm (*51*)] of the data to a square hyperbola. In the absence of DNA, kinetic parameters were $V_{max} = 0.30 \pm 0.02$ μM ADP/min and $K_M = 36 \pm 9$ μM ATP. The corresponding parameters obtained in the presence of heteroduplex were $V_{max} = 1.20 \pm 0.06$ μM ADP/min and $K_M = 33 \pm 6$ μM ATP. (Panel B) inhibition of MutS ATPase by ADP (●), ATPγS (■), and AMPPNP (□). The ATPase activity of 300 nM MutS (monomer concentration) was measured at 50 μM ATP in the presence of the indicated concentrations of inhibitors. The data have been fit using eq 1 with $K_{i,ADP} = 40 \pm 10$ μM, $K_{i,AMPPNP} = 3.5 \pm 0.4$ μM, and $K_{i,ATP\gamma S} = 4.2 \pm 0.3$ μM.

of ATP hydrolysis was determined by chromatography of 1 μL of quenched samples PEI−Cellulose plates (EM Science, Gibbstown, NJ) which were developed in 0.3 M KPO_4, pH 7.0. Dried plates were phosphoimaged overnight and optically scanned using a STORM imager system, and the resultant data were analyzed using Imagequant software (Molecular Dynamics). Initial steady-state rates of ATP hydrolysis were determined by least-squares analysis of the linear portion of progress curve.

Pre-steady-state experiments were performed using a KinTek chemical quench apparatus (KinTek Corp., State College, PA). To promote solubility at the high MutS concentrations required for these experiments, the time courses were measured in 25 mM Tris-HCl, pH 7.6, 100 mM KCl, 5 mM $MgCl_2$, 100 μg/mL BSA, 10% (v/v) glycerol. In addition, the syringe containing the MutS was kept at 4.0 °C by a jacket of ice prior to equilibration at the reaction temperature (≥3 min) at 25 °C. Reactions were quenched with 0.33% SDS (final concentration) to liberate bound nucleotide. The extent of ATP hydrolysis was determined by thin-layer chromatography as described above.

Gel Filtration Analysis. Gel filtration experiments were performed using a Waters Liquid Chromatography system

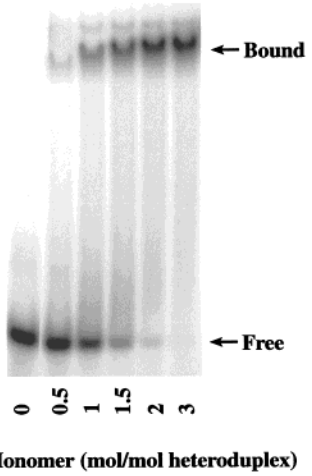

FIGURE 2: MutS preparations are fully active in mismatch binding. Reactions (20 μL) contained 1 pmol of a 5′-^{32}P-end-labeled 31 base pair G−T heteroduplex and MutS as indicated. After incubation at 25 °C for 10 min, reactions were analyzed by gel shift assay (Materials and Methods) to score free and MutS-bound heteroduplex.

(Millipore Corp., Milford, MA) with a Superose 6 HR 10/30 column (Amersham Pharmacia Biotech Inc., Piscataway, NJ). Chromatography was in 25 mM Tris-HCl, pH 7.6, 150 mM KCl, 0.1 mM EDTA at a flow rate of 0.5 mL/min, and the elution profile was monitored by the absorbance at 280 nm. The MutS samples were prepared by serial dilution of the 3 μM sample and allowed to equilibrate on ice for at least 30 min. The column was calibrated using the following molecular mass standards (Sigma, St. Louis, MO): thyroglobin (669 kDa), apoferritin (443 kDa), β-amylase (200 kDa), alcohol dehydrogenase (150 kDa), BSA (66 kDa), and carbonic anhydrase (29 kDa). A plot of ln(MW) versus retention time was linear and fit to the equation of ln(MW) $= 21.3 - 0.29t$, where t is retention time in minutes.

RESULTS

ATP Hydrolysis by E. coli MutS in the Absence of DNA. Bacterial MutS proteins and its eukaryotic homologues have been reported to have a slow ATPase activity (*1*, *24*−*28*, *36*) which yields free phosphate and ADP as products. We have examined the kinetics of ATP hydrolysis by *E. coli* MutS. As shown in Figure 1A, the ATP hydrolytic rate obeys Michaelis−Menten kinetics with a maximal hydrolysis rate (k_{cat}) of 1.0 ± 0.1 ADP min^{-1} per MutS monomer equivalent and a K_M of 36 ± 9 μM. These parameters are in qualitative agreement with those obtained with *Salmonella typhimurium* MutS [$k_{cat} = 0.3$ min^{-1}, $K_M = 7$ μM (*24*)] and His_6-tagged *E. coli* MutS [$k_{cat} = 7$ min^{-1}, $K_M = 15$ μM (*37*)]. ATP turnover by eukaryotic MutS homologues is also similarly slow (*25*, *26*, *28*).

The modest ATP hydrolytic turnover number for bacterial MutS is not due to the presence of a significant fraction of inactive protein in the preparations used here. Surface plasmon resonance spectroscopy analysis has previously shown that *E. coli* MutS binds to a G−T mismatch as a dimer in the absence of ATP (*11*), and similar results have been obtained with the *Thermus aquaticus* protein (*21*). The fraction of active MutS was therefore determined by titration assay in the absence of nucleotide at protein and DNA concentrations where binding is near-stoichiometric. Gel

mobility shift analysis (Figure 2) under these conditions demonstrated that 2 molar equiv of MutS monomer was sufficient to shift 0.94 mol of a 31 base pair G−T heteroduplex. Therefore, the MutS preparations used in this study were better than 90% active with respect to mismatch recognition.

Genetic analysis has indicated that the nucleotide hydrolytic center of bacterial MutS is required for mismatch repair in vivo (*24*, *30*), and poorly hydrolyzed ATP analogues have been shown to inhibit steps of the mismatch repair reaction in vitro. ATPγS inhibits the MutS-, MutL-, and ATP-dependent activation of the MutH d(GATC) endonuclease (*1*) and, unlike ATP, fails to support DNA loop extrusion by MutS (*11*). Excess AMPPNP over ATP has also been found to halt MutS-mediated DNA loop growth. We have therefore examined the nature of the inhibition of MutS ATPase activity by these analogues. Both ATPγS and AMPPNP inhibited ATP hydrolysis by MutS with a similar concentration dependence (Figure 1B), and in both cases, inhibition was consistent with the simple competitive mechanism described by eq 1.

$$V = \frac{k_{cat}[\text{MutS}][\text{ATP}]}{K_M\left(\frac{[\text{I}]}{K_i} + 1\right) + [\text{ATP}]} \quad (1)$$

Using K_M and k_{cat} values obtained from the fit shown in Figure 1A, the inhibition constants were calculated as $K_{i,ATP\gamma S} = 4.2 \pm 0.3$ μM and $K_{i,AMPPNP} = 3.5 \pm 0.4$ μM. Inhibition by ADP and P_i products was also examined. Inhibition by the former was also competitive with a $K_{i,ADP} = 40 \pm 10$ μM (Figure 1B). Interestingly, inorganic phosphate did not inhibit ATP hydrolysis at concentrations as high as 50 mM, and, surprisingly, did not potentiate inhibition by ADP (not shown). The latter finding is relevant to buffer effects observed during electron microscopy of MutS·heteroduplex complexes. The previously reported reduction in the rate of DNA loop extrusion by MutS observed in phosphate as opposed to HEPES buffer (*11*) is presumably a consequence phosphate effects on MutS−DNA interactions rather than a product inhibition effect.

Modulation of MutS ATPase Activity by Heteroduplex and Homoduplex DNAs. Previous reports on the ATPase activity of bacterial MutS did not reveal any potential effects of DNA cofactors on ATP hydrolysis (*1*, *37*). These observations are in contrast to results obtained with eukaryotic MutS homologues, where DNA has been reported to have modest to substantial effects on ATPase activity depending on the source of the protein and presence or absence of a mismatch within the DNA cofactor (*26*−*28*, *33*, *36*). To clarify this question in the case of the *E. coli* protein, we have also examined the rate of ATP hydrolysis in the presence of an excess of a 20 bp duplex containing a centrally located G−T mismatch, under conditions where virtually all of the MutS is DNA-bound (*9*). As shown in Figure 1A, the presence of the 20mer heteroduplex increased the maximal rate of ATP hydrolysis 4-fold, corresponding to a turnover rate of 4.2 ± 0.3 ADP min^{-1} per MutS monomer equivalent. However, the K_M for ATP was unchanged with a value of 33 ± 6 μM. A similar enhancement in the rate of ATP hydrolysis by heteroduplex DNA has been observed with human MutSα (*26*, *28*).

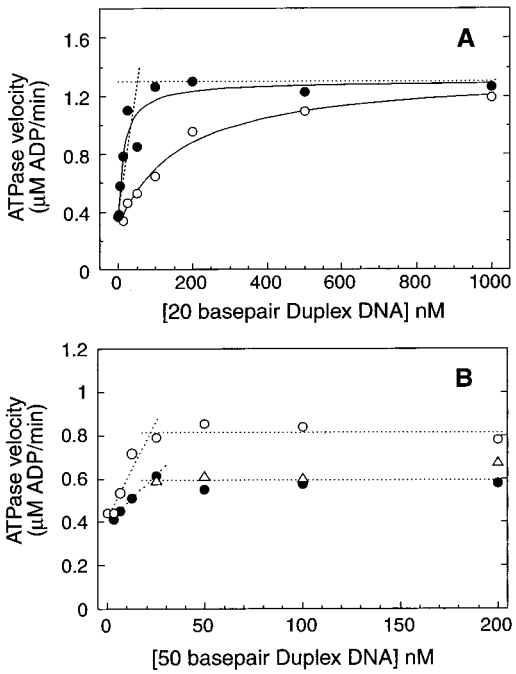

FIGURE 3: ATPase activation by heteroduplex and homoduplex DNA. Steady-state ATPase velocity was measured with 300 nM MutS and 200 μM ATP in the presence of (panel A) 20 base pair homo- or G−T heteroduplex DNA as indicated or (panel B) 50 base pair homo- or G−T heteroduplex. (●) Heteroduplex cofactor; (○) homoduplex cofactor; (△) 25 nM heteroduplex cofactor with the indicated concentration of homoduplex cofactor.

To determine whether ATPase activation by DNA is dependent on the presence of a mismatched base pair, activation by the 20 base pair G−T heteroduplex mentioned above and an otherwise identical homoduplex were compared. As shown in Figure 3A, the 20 bp homoduplex was sufficient to activate ATP hydrolysis by MutS, albeit at a higher DNA concentration than the G−T heteroduplex. Relative specificities for activation by these two DNAs cannot be determined under the experimental conditions of Figure 3A due to the fact that binding of the heteroduplex DNA cofactor is stoichiometric or nearly so (dashed lines) at the concentrations used. In fact, the effect of added heteroduplex appears to saturate at 50 ± 20 nM heteroduplex for 300 nM MutS monomer. Since this apparent stoichiometry (6 ± 2) has been observed with several independent MutS preparations (not shown) and since, as described above, these preparations are completely active with respect to mismatch binding, this stoichiometry is not due to presence of inactive protein. This point will be considered below.

Interestingly, the degree of stimulation by DNA cofactors can be sensitive to the chain length of the DNA cofactor. Fifty base pair oligonucleotides also stimulate MutS ATPase, but to a lesser extent than the 20 base pair cofactors (Figure 3B). Moreover, the degree of stimulation is sensitive to the presence of a mismatch, with the heteroduplex molecule yielding only a 1.5-fold stimulation compared to a 2-fold stimulation for the corresponding homoduplex molecule. A similar level of ATPase stimulation has been observed upon addition of homopolymeric DNA substrates (K. Bjornson and P. Modrich, data not shown), consistent with the DNA length effect on MutS k_{cat} saturating at 50 base pairs. The 50 base pair homo- and heteroduplex DNA cofactors both appear to bind stoichiometrically under the conditions used

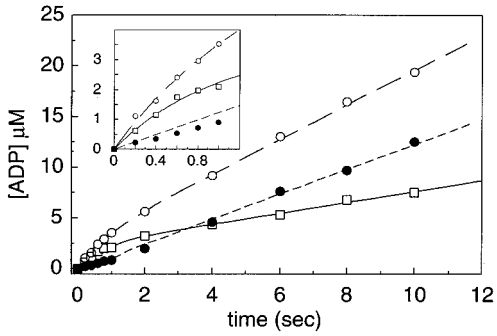

FIGURE 4: Pre-steady-state analysis of ATP hydrolysis by MutS. Pre-steady-state analysis was performed as described under Materials and Methods. MutS (60 μM monomer) in the absence of DNA (□) or in the presence of 10 μM 20 base pair homoduplex (○) or G−T heteroduplex (●) was mixed with an equal volume of 200 μM ATP. Data were fit by a Marquardt nonlinear least-squares routine to the equation: $[ADP] = Amp[1 - \exp(-k_{obs}t)] + tV$, where Amp is the burst amplitude, k_{obs} is the rate constant for the burst phase, and V is the steady-state rate of ATP hydrolysis. In the absence of DNA cofactor (□), ATP hydrolysis shows a burst of ADP production with Amp = 2.3 ± 0.2 μM, k_{obs} = 82 ± 11 min^{-1}, and a steady-state rate of 32 ± 3 μM ADP/min. MutS preincubated with homoduplex (○) also displayed a burst of ADP production with Amp = 2.5 ± 0.3 μM, k_{obs} = 78 ± 12 min^{-1}, and a steady-state rate of 103 ± 2 μM ADP/min. Preincubation of MutS with heteroduplex DNA (●) abolished the burst of ADP production and had a steady-state rate of ATP hydrolysis of 74 ± 1 μM ADP/min.

in these experiments, precluding determination of the degree of specificity for the two molecules. However, competition experiments in which 50mer homo- and heteroduplexes were present in the same reaction (Figure 3B) yielded the reduced degree of activation that was characteristic of heteroduplex alone, even when the homoduplex was present in 8-fold molar excess. Therefore, the 50 base pair homo- and heteroduplexes appear to bind competitively, and as observed with the 20 base pair DNA cofactors, the heteroduplex outcompetes the homoduplex.

It is also important to note that the apparent DNA:MutS stoichiometry for ATPase activation by 50 base pair DNAs is about half that observed with 20 base pair duplexes, with 25 nM DNA molecules sufficient to completely activate 300 nM MutS monomer. This stoichiometry is consistent with a site size of approximately 20 base pairs for binding of the MutS oligomer, a value similar to that obtained by footprint analysis (*9*, *12*, *22*).

Pre-Steady-State ATP Hydrolysis by MutS. To further clarify the nature of activation of the MutS ATPase by the binding of homoduplex and heteroduplex DNA cofactors, we have used pre-steady-state chemical quench methods to examine the initial turnover of ATP that precedes entry into steady-state hydrolysis (Figure 4). In these experiments 30 μM MutS monomer (final concentration) either alone or in the presence of 5 μM 20 base pair homo- or heteroduplex DNA was rapidly mixed with 100 μM ATP. In the absence of DNA, MutS showed a rapid burst of ATP hydrolysis (k_{obs} = 82 ± 11 min^{-1} with an amplitude of 2.3 ± 0.2 μM) which preceded a slow steady-state phase governed by a rate constant of 1.1 ± 0.1 min^{-1}. This demonstrates that the rate-limiting step for ATPase turnover occurs after hydrolysis. Therefore, under conditions of saturating nucleotide, the MutS hydrolytic center will exist predominantly in an ADP-bound form. It is also apparent from this analysis that not all of the MutS monomer (30 μM) turns over during the first round of ATP hydrolysis. A nonunity burst amplitude of this sort might be attributed to the presence of inactive MutS, but as noted above, the preparations used in this work were fully active with respect to mismatch recognition. Furthermore, the substoichiometric burst amplitude observed was independent of MutS preparation and essentially invariant with reaction temperature from 4 to 25 °C (data not shown). An alternate explanation attributes the substoichiometric burst to the presence of multiple classes of nucleotide binding sites within the MutS oligomer. Some evidence for assembly of *E. coli* MutS has been presented (*19*), and this issue is considered further below.

In the presence of 5 μM 20 base pair homoduplex, the initial burst rate and amplitude of ATP hydrolysis were unaffected (k_{obs} = 78 ± 12 min^{-1}, Amp = 2.5 ± 0.3 μM ADP) as compared to single turnover in the absence of DNA. However, the subsequent steady-state turnover rate was increased to 3.4 ± 0.1 min^{-1}, similar to the value, 4 min^{-1}, obtained above under steady-state conditions at saturating DNA cofactor (Figure 3A). Binding of homoduplex DNA, therefore, increases the steady-state rate of ATP hydrolysis solely by enhancing the rate of one or more steps that occur after hydrolysis.

In contrast to the mechanism of activation of nucleotide hydrolysis by homoduplex DNA, the presence of a mismatch within the DNA cofactor alters the kinetic mechanism of ATP hydrolysis (Figure 4). The presence of an otherwise identical 20 base pair duplex containing a centrally located G−T was sufficient to abolish the burst phase of ATP hydrolysis, indicating that the rate-limiting step either precedes or corresponds to the chemical hydrolytic step. Thus, while the apparent level of stimulation of ATP turnover by the 20 base pair homo- and heteroduplexes is similar (Figures 3A and 4), the kinetic mechanisms of the corresponding hydrolytic reactions are distinct.

ATP-Dependent Assembly of MutS Oligomers. The apparent stoichiometry of DNA activation of the MutS ATPase and the substoichiometric burst amplitude of ATP hydrolysis during the first turnover suggest heterogeneity of nucleotide and DNA binding sites within the homooligomeric MutS protein. We have used size exclusion gel chromatography to assess MutS assembly as a function of protein concentration in the absence and presence of ATP (Figure 5). In the absence of nucleotide at the lowest concentration tested (0.75 μM monomer), MutS eluted as two peaks (panel A). The later eluting peak at 32.2 min has an apparent molecular mass of 160 kDa (Materials and Methods), corresponding to a MutS 1.7mer, an observation consistent with previous evidence for dimerization of the MutS polypeptide (*11*, *19*−*21*). The retention time of the earlier eluting peak (27.4 min) corresponds to an apparent molecular mass of 580 kDa, that expected for a MutS hexamer, although assignment of this aggregation state must be regarded as tentative in the absence of information on the frictional coefficient of this species. Doubling of the protein concentration to 1.5 μM reduced the fraction of MutS present in the later eluting peak, which had the apparent molecular mass of a 200 kDa dimer, with the remainder of the material eluting at the expected position of a hexamer. At a concentration of 3 μM (monomer), MutS eluted as a single species of apparent hexameric structure (Figure 5A). Furthermore, when gel filtration was performed

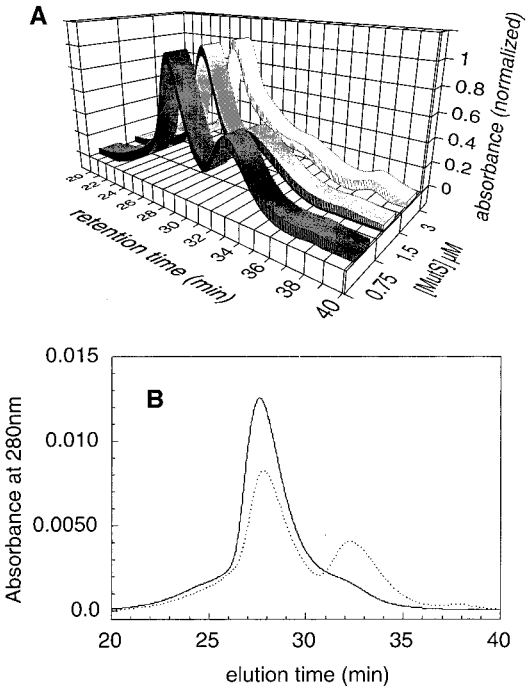

FIGURE 5: MutS assembles in a concentration-dependent manner, and assembly is promoted by ATP binding. (Panel A) MutS at 0.75, 1.5, and 3.0 μM (monomer concentration) was subjected to gel filtration as described under Materials and Methods. Elution profiles are normalized to permit comparison at the different protein concentrations. (Panel B) Elution profile at 0.75 μM MutS in the absence (dashed line) and after preincubation with 100 μM ATP in the absence of Mg^{2+} (solid line).

at the 30 μM MutS concentration employed in the pre-steady-state experiments described above, essentially all of the protein eluted with a retention time expected for the putative hexamer (data not shown).

This chromatographic behavior is indicative of an assembling system. Moreover, the MutS oligomerization appears to be fairly well-defined because the retention time of the higher molecular weight species was invariant with increased protein concentration over the range tested. MutS assembly visualized in this manner may be relevant to the biological activity of the protein because the presence of ATP (in the absence of Mg^{2+}) promoted oligomerization as shown in Figure 5B. At the lowest MutS concentration examined (750 nM), and in the presence of nucleotide, the protein eluted as a single species with the apparent molecular mass of a hexamer. Preincubation of the protein with ADP or ATP in the presence of Mg^{2+} resulted in a slight shift of the later eluting peak to 31.5 min, corresponding to an apparent dimer (data not shown). Therefore, ATP binding rather than hydrolysis drives the MutS assembly shown in Figure 5. As considered below, this behavior is similar to that observed with several of the hexameric DNA helicases.

DISCUSSION

We have shown that the ATPase activity of bacterial MutS is DNA-modulated. This finding is consistent with the DNA stimulation observed in the case of several of the eukaryotic MutS homologues which have recently been characterized. The ATPase activities of yeast (yMutSα) and human (hMutSα, hMutSβ) MutS homologues have all been shown to be stimulated by the binding of homoduplex DNA (*26, 28, 33, 38*). However, the relative ATPase activation by the binding of heteroduplex DNA varies between these homologous proteins. The mechanistic relevance of the apparent differences in ATPase stimulation by DNA cofactors will require further characterization. Certainly the different solution conditions used in the various studies could play a factor. In the case of hMutSα, the relative level of ATPase stimulation by hetero- and homoduplex DNA cofactors for hMutSα has been shown to be sensitive to ionic conditions (*28*).

The variable degree of steady-state activation of the *E. coli* MutS ATPase by homo- and heteroduplex DNA can be understood in terms of the pre-steady-state results shown in Figure 4. In the absence of DNA, the first hydrolytic turnover is fast ($k_{obs} = 82$ min^{-1}) compared to the slow steady-state rate ($k_{obs} = 1.1$ min^{-1} per monomer equivalent). The rate-limiting step for ATPase turnover therefore occurs after hydrolysis. Such behavior is common for enzymatic reactions where turnover is limited by the rate of product release. In such a mechanism, the effect of homoduplex DNA binding by MutS is to accelerate the release of ADP. In fact, the kinetics of the initial ATP hydrolytic event preceding the steady-state are unaffected by the binding of homoduplex DNA ($k_{obs} = 78$ min^{-1}). However, a different situation holds when MutS is bound at a mismatch. In this case, the initial ATP hydrolytic event is no longer fast, and no burst of ADP formation occurs, indicating that the rate-limiting step for turnover now corresponds to hydrolysis or occurs prior to this step. Thus, the nucleotide hydrolytic center of MutS free in solution or bound to perfectly paired sequences will exist predominantly in the ADP form (rate-limiting step after hydrolysis); the hydrolytic center of MutS bound at a mismatch will be occupied predominantly by ATP (rate-limiting step at or before hydrolysis). This relatively long-lived MutS·ATP·mismatch complex may be the species that serves to recruit MutL since the MutS-dependent binding of MutL to heteroduplex DNA in the *E. coli* and yeast systems has been shown to depend on ATP binding but not ATP hydrolysis (*11, 12, 39*).

Previous work has shown that ATP binding is sufficient to reduce the affinity of bacterial MutS and human MutSα for a mismatch (*11, 12, 26, 29, 31*). Furthermore, both bacterial MutS and human MutSα leave the mismatch in the presence of ATP by movement along the DNA contour (*11, 29, 34*). There are, however, differences in the literature with respect to the requirement for ATP hydrolysis during the process of movement along the helix: while one model posits that hydrolysis occurs during movement along the helix (*11, 29*), the other postulates that hydrolysis only occurs after release from the DNA (*34*). Nevertheless, if movement away from the mismatch necessarily precedes hydrolysis, then initial movement away from the mispair may well correspond to the slow step in the ATP hydrolytic cycle. Such a mechanism predicts tight coupling between movement on DNA and ATP hydrolysis. Indeed, it has been found that steric blocking of the termini of a 41 base pair heteroduplex with biotin-bound avidin reduces the ATPase activity of human MutSα as compared to that observed with unblocked DNA (*34*). In addition, an inverse correlation has been reported with respect to the strength of binding of heteroduplex DNA and the degree of ATPase stimulation for the yeast MutS homologue MSH1 (*36*). These observations are

also consistent with a mechanism in which release from the mismatch is a prerequisite for ATP hydrolysis. In view of the sequence and functional conservation of MutS homologues, similarities in mechanism would not be surprising.

The roles of ATP binding and hydrolysis are likely to be multifarious. In addition to function of the nucleotide in MutS-dependent recruitment of MutL to the heteroduplex and movement of MutS along the helix, we have found that ATP binding also promotes assembly of MutS oligomers. Previous studies of bacterial MutS activities have indicated that a dimer is sufficient for mismatch recognition in the absence of ATP (*11*, *21*), but higher order aggregates have been observed by electron microscopy of *E. coli* MutS·DNA complexes at high protein to DNA ratios in the presence of ATP (*11*). Although the physiologically relevant MutS aggregation state has yet to be defined, our gel filtration data (Figure 5) are most consistent with the limiting species being a tetramer or hexamer. Therefore, multiple ATP binding sites exist within a MutS multimer, and, as noted above, these sites are not kinetically equivalent. There is extensive precedent for the existence of multiple classes of nucleotide binding site within homooligomeric proteins that move along the DNA helix. For example, the *E. coli* DnaB helicase (*40*), the Rho transcription termination factor (*41*), and the phage T7 gene 4 helicase/primase(*42*) are all homooligomeric proteins with tight and weak nucleotide binding sites, which is indicative of communication between nucleotide binding centers. Of particular relevance to our finding that ATP promotes MutS assembly are the hexameric protein systems phage T7 gene 4 helicase/primase (*43*), *E. coli* Rho (*44*), SV40 Large T antigen (*45*, *46*), and phageT4 gene 41 helicase (*47*). Assembly of the functional hexamer for each of these activities is linked to nucleoside triphosphate binding rather than hydrolysis, as we have observed for MutS.

It is also noteworthy in this regard that the apparent stoichiometry of DNA oligonucleotide activation of MutS ATPase activity under steady-state conditions (Figure 3) indicates that a 20 pair duplex is sufficient to activate 6 ± 2 MutS monomers, whereas a 50 base pair oligonucleotide saturates stimulation at a ratio of 12 ± 3 MutS monomers. These data indicate that the occluded site size of a MutS oligomer is approximately 20 base pairs, a size essentially identical to the binding site size deduced in footprinting experiments (*9*, *12*, *22*).

Despite the finding that the MutS preparations used in this study are fully active in mismatch binding, pre-steady-state burst experiments (Figure 4) show that only a fraction of MutS monomers turn over during the first round of hydrolysis. The simplest interpretation of this nonunity burst amplitude is functional heterogeneity within the MutS oligomer. A similar effect has been observed with the hexameric *E. coli* RuvB protein, a protein that translocates along DNA in an ATP-dependent manner (*48*). Pre-steady-state analysis of RuvB has demonstrated a substoichiometric burst amplitude for ATP hydrolysis of 2 ATP/hexamer (*49*). Although there is qualitative similarity between this finding and the substoichiometric amplitude described here, the apparent stoichiometry for MutS shown in Figure 4 is a burst of 1 ATP/12 MutS monomers. It is clear that additional studies will be necessary to define the cooperative behavior of ATP binding sites.

A growing number of DNA translocating proteins have been shown to encircle either one or both strands of the helix including T7 gene 4 helicase/primase, *E. coli* DnaB helicase, *E. coli* RuvB, and SV40 Large T antigen (*50*). The inability of human MutSα to dissociate from small heteroduplexes in which the DNA ends have been physically blocked has led to the suggestion that MutS homologues may also be capable of forming a ring-like structure around duplex DNA (*29*, *34*). Preliminary experiments also indicate that *E. coli* MutS also becomes physically trapped on end-blocked heteroduplexes, with the formation of these dissociation-resistant complexes depending on ATP hydrolysis (L. Blackwell and P. Modrich, unpublished results). Such a mobile clamp mechanism provides an obvious means by which MutS would be able to transmit the presence of a mismatched base pair along the DNA contour to the strand signal where excision initiates (*3*). The ATP-driven assembly of MutS that we have observed could contribute to the formation of a ring-like structure that confers processivity to a translocating MutS·MutL complex.

REFERENCES

1. Au, K. G., Welsh, K., and Modrich, P. (1992) *J. Biol. Chem. 267*, 12142−12148.
2. Yamaguchi, M., Dao, V., and Modrich, P. (1998) *J. Biol. Chem. 273*, 9197−9201.
3. Dao, V., and Modrich, P. (1998) *J. Biol. Chem. 273*, 9202−9207.
4. Meselson, M. (1988) in *Recombination of the Genetic Material* (Low, K. B., Ed.) pp 91−113, Academic Press, San Diego, CA.
5. Radman, M., Matic, I., Halliday, J. A., and Taddei, F. (1995) *Philos. Trans. R. Soc. London B, Biol. Sci. 347*, 97−103.
6. Kolodner, R. (1996) *Genes Dev. 10*, 1433−1442.
7. Modrich, P., and Lahue, R. (1996) *Annu. Rev. Biochem. 65*, 101−133.
8. Jiricny, J. (1998) *EMBO J. 17*, 6427−6436.
9. Su, S.-S., Lahue, R. S., Au, K. G., and Modrich, P. (1988) *J. Biol. Chem. 263*, 6829−6835.
10. Parker, B. O., and Marinus, M. G. (1992) *Proc. Natl. Acad. Sci. U.S.A. 89*, 1730−1734.
11. Allen, D. J., Makhov, A., Grilley, M., Taylor, J., Thresher, R., Modrich, P., and Griffith, J. D. (1997) *EMBO J. 16*, 4467−4476.
12. Grilley, M., Welsh, K. M., Su, S.-S., and Modrich, P. (1989) *J. Biol. Chem. 264*, 1000−1004.
13. Galio, L., Bouquet, C., and Brooks, P. (1999) *Nucleic Acids Res. 27*, 2325−2331.
14. Cooper, D. L., Lahue, R. S., and Modrich, P. (1993) *J. Biol. Chem. 268*, 11823−11829.
15. Grilley, M., Griffith, J., and Modrich, P. (1993) *J. Biol. Chem. 268*, 11830−11837.
16. Lahue, R. S., Au, K. G., and Modrich, P. (1989) *Science 245*, 160−164.
17. Fang, W., and Modrich, P. (1993) *J. Biol. Chem. 268*, 11838−11844.
18. Umar, A., Boyer, J. C., Thomas, D. C., Nguyen, D. C., Risinger, J. I., Boyd, J., Ionov, Y., Perucho, M., and Kunkel, T. A. (1994) *J. Biol. Chem. 269*, 14367−14370.
19. Su, S.-S., and Modrich, P. (1986) *Proc. Natl. Acad. Sci. U.S.A. 83*, 5057−5061.
20. Takamatsu, S., Kato, R., and Kuramitsu, S. (1996) *Nucleic Acids Res. 24*, 640−647.
21. Biswas, I., Ban, C., Fleming, K. G., Qin, J., Lary, J. W., Yphantis, D. A., Yang, W., and Hsieh, P. (1999) *J. Biol. Chem. 274*, 23673−23678.
22. Biswas, I., and Hsieh, P. (1997) *J. Biol. Chem. 272*, 13355−13364.

23. Jiricny, J., Su, S.-S., Wood, S. G., and Modrich, P. (1988) *Nucleic Acids Res. 16,* 7843−7854.
24. Haber, L. T., and Walker, G. C. (1991) *EMBO J. 10,* 2707−2715.
25. Alani, E., Sokolsky, T., Studamire, B., Miret, J. J., and Lahue, R. S. (1997) *Mol. Cell. Biol. 17,* 2436−2447.
26. Gradia, S., Acharya, S., and Fishel, R. (1997) *Cell 91,* 995−1005.
27. Iaccarino, I., Marra, G., Palombo, F., and Jiricny, J. (1998) *EMBO J. 17,* 2677−2686.
28. Blackwell, L. J., Bjornson, K. P., and Modrich, P. (1998) *J. Biol. Chem. 273,* 32049−32054.
29. Blackwell, L. J., Martik, D., Bjornson, K. P., Bjornson, E. S., and Modrich, P. (1998) *J. Biol. Chem. 273,* 32055−32062.
30. Wu, T. H., and Marinus, M. G. (1994) *J. Bacteriol. 176,* 5393−5400.
31. Drummond, J. T., Li, G.-M., Longley, M. J., and Modrich, P. (1995) *Science 268,* 1909−1912.
32. Iaccarino, I., Palombo, F., Drummond, J., Totty, N. F., Hsuan, J. J., Modrich, P., and Jiricny, J. (1996) *Curr. Biol. 6,* 484−486.
33. Alani, E. (1996) *Mol. Cell. Biol. 16,* 5604−5615.
34. Gradia, S., Subramanian, D., Wilson, T., Acharya, S., Makhov, A., Griffith, J., and Fishel, R. (1999) *Mol. Cell 3,* 255−261.
35. Gill, S. C., and von Hippel, P. H. (1989) *Anal. Biochem. 182,* 319−326.
36. Chi, N. W., and Kolodner, R. D. (1994) *J. Biol. Chem. 269,* 29993−29997.
37. Worth, L., Jr., Bader, T., Yang, J., and Clark, S. (1998) *J. Biol. Chem. 273,* 23176−23182.
38. Wilson, T., Guerrette, S., and Fishel, R. (1999) *J. Biol. Chem. 274,* 21659−21664.
39. Habraken, Y., Sung, P., Prakash, L., and Prakash, S. (1998) *J. Biol. Chem. 273,* 9837−9841.
40. Bujalowski, W., and Klonowska, M. M. (1993) *Biochemistry 32,* 5888−5900.
41. Geiselmann, J., and von Hippel, P. H. (1992) *Protein Sci. 1,* 850−860.
42. Patel, S. S., and Hingorani, M. M. (1995) *Biophys. J. 68,* 186S−189S, discussion 189S−190S.
43. Egelman, H. H., Yu, X., Wild, R., Hingorani, M. M., and Patel, S. S. (1995) *Proc. Natl. Acad. Sci. U.S.A. 92,* 3869−3873.
44. Finger, L. R., and Richardson, J. P. (1982) *J. Mol. Biol. 156,* 203−219.
45. Mastrangelo, I. A., Hough, P. V., Wall, J. S., Dodson, M., Dean, F. B., and Hurwitz, J. (1989) *Nature 338,* 658−662.
46. Mastrangelo, I. A., Bezanilla, M., Hansma, P. K., Hough, P. V., and Hansma, H. G. (1994) *Biophys. J. 66,* 293−298.
47. Dong, F., Gogol, E. P., and von Hippel, P. H. (1995) *J. Biol. Chem. 270,* 7462−7473.
48. West, S. C. (1997) *Annu. Rev. Genet. 31,* 213−244.
49. Marrione, P. E., and Cox, M. M. (1995) *Biochemistry 34,* 9809−9818.
50. Hingorani, M. M., and O'Donnell, M. (1998) *Curr. Biol. 8,* R83−86.
51. Marquardt, D. W. (1963) *J. Soc. Indust. Appl. Math. 11,* 431−441.

BI992286U